

Search for differences between radio-loud and radio-quiet gamma-ray pulsar populations with Fermi-LAT data

E.V. Sokolova and G.I. Rubtsov

sokol@ms2.inr.ac.ru, grisha@ms2.inr.ac.ru

Institute for Nuclear Research of the Russian Academy of Sciences, Moscow 117312, Russia

ABSTRACT

Observations by Fermi-LAT have enabled us to explore the population of non-recycled gamma-ray pulsars with a set of 112 objects. It was recently noted that there are apparent differences in the properties of radio-quiet and radio-loud subsets. In particular, the average observed radio-loud pulsar is younger than the radio-quiet one and is located at smaller Galactic latitude. Even so, the analysis based on the full list of pulsars may suffer from selection effects. Namely, most radio-loud pulsars are first discovered in the radio band, while radio-quiet ones are found using the gamma-ray data. In this work we perform a blind search for gamma-ray pulsars using the Fermi-LAT data alone, using all point sources from the 3FGL catalog as the candidates. Unlike our previous work, the present catalog is constructed with a semi-coherent method based on the time-differencing technique and covers the full range of characteristic ages down to 1 kyr. The search resulted in a catalog of 40 non-recycled pulsars, 25 of which are radio-quiet. All pulsars found in the search were previously known gamma-ray pulsars. We find no statistically significant differences in age and Galactic latitude distributions for the radio-loud and radio-quiet pulsars, while the rotation period distributions are marginally different with statistical probability of 4×10^{-3} . The fraction of radio-quiet pulsars is estimated as $\epsilon_{RQ} = 63 \pm 8\%$. The results are in agreement with the predictions of the outer magnetosphere models, while the Polar cap models are disfavored.

Subject headings: pulsars: general — gamma rays: stars

1. Introduction

The number of known gamma-ray pulsars has grown rapidly since the Fermi Large Area Telescope (LAT) started taking data in August 2008. At present 205¹ gamma-ray pulsars are identified, including 112 non-recycled pulsars. The latter includes 61 radio-loud pulsars and 51 radio-quiet ones, see Caraveo (2014); Grenier & Harding (2015) for a review. With the only exception of Geminga (Halpern & Holt 1992; Bertsch et al. 1992), the detection of the radio-quiet pulsars became possible only with the sensitivity of Fermi-LAT. High-performance numerical methods

were designed and implemented based on the time-differencing technique (Atwood et al. 2006; Abdo et al. 2009a; Saz Parkinson et al. 2010; Pletsch et al. 2012a,b; Clark et al. 2015).

With the statistics in hands one may raise questions on the model of the gamma-ray emission and corresponding mechanism of the radio-quietness. Two general classes of the pulsar gamma-ray emission models are discussed. The first class includes the so-called Polar cap (PC) models (Sturrock 1971). In these models gamma rays are produced by electrons and positrons accelerated in the polar cap region near the surface of the neutron star. In the PC models the gamma-ray and radio beams are generally co-aligned. The latter is considered narrower than the former and therefore some of the pulsars are observed as radio-quiet (Sturmer &

¹<https://confluence.slac.stanford.edu/display/GLAMCOG/Public+List+of+LAT-Detected+Gamma-Ray+Pulsars>

Dermer 1996). Moreover, in the PC models the fraction of the radio-quiet pulsars depends on the pulsar’s age (Gonthier et al. 2002). In the second class of models the gamma-ray emission is produced in the outer magnetosphere (OM) of the pulsar (Cheng et al. 1986; Perera et al. 2013). In the OM models the radio-quietness finds a geometrical description as the gamma-ray and radio-beams orientations are naturally diverse. Moreover, beam geometry within the OM models may serve as a consistent description of recent Chandra and XMM-Newton observations of gamma-ray pulsars (Marelli et al. 2015). The latter showed that on average radio-quiet pulsars have higher gamma-ray-to-x-ray flux ratio than radio-loud ones.

It was noted that the observed fraction of the radio-quiet objects is relatively small for young pulsars (Ravi et al. 2010). This observation may be interpreted in terms of evolution of the radio-beam solid angle (Ravi et al. 2010; Watters & Romani 2011). Alternatively this may be an effect of the observational selection bias (Caraveo 2014). While radio-quiet pulsars are discovered in a blind search with gamma-ray data, there are multiple ways to find radio-loud pulsars. The latter may be found either in radio surveys or with follow-up observations of gamma-ray sources. In most cases the gamma-ray pulsations of radio-loud pulsars are found with ephemerides from radio observations. Nevertheless there are pulsars with pulsed radio-emission detected following the gamma-ray pulsations.

In this *Paper* we construct a less biased catalog of the gamma-ray selected pulsars by performing a blind search for gamma-ray pulsars using the Fermi LAT data alone. The search is more extensive with respect to our preceding blind search (Rubtsov & Sokolova 2015). With the novel efficient semi-coherent method a complete range of characteristic ages starting from 1 kyr is covered. No radio or optical observation data are used.

The paper is organized as follows. Fermi-LAT data selection and preparation procedures are explained in Section 2. The implementation details of the semi-coherent method are given in Section 3. The catalog of the gamma-ray selected pulsars, comparison of radio-quiet and radio-loud gamma-ray pulsar populations and comparison of the results to the predictions of the pulsar emission mod-

els are presented in Section 4.

2. Data

The paper is based on publicly-available weekly all-sky Fermi-LAT data for the time period from 2008 August 4 till 2015 March 3 (Mission elapsed time from 239557418 to 447055673) (Atwood et al. 2009)². We select SOURCE class events from Reprocessed Pass 7 data set with energies from 100 MeV to 300 GeV. The standard quality cuts are applied using the *Fermi Science Tools v9r32p5* package. These include 100° and 52° upper constraints for zenith angle and satellite rocking angle, respectively.

We search for pulsations using the location of each of 3008 point sources from the Fermi LAT 4-year Point Source Catalog (3FGL) (Acero et al. 2015). The requirement of blindness to everything except gamma-ray emission binds us to the coordinates from the 3FGL catalog. Although the precision of the gamma-ray source positioning is one of the factors limiting sensitivity of the scan (Pletsch et al. 2012a) we did not scan over the sky location due to computational complexity. This has an effect on the sensitivity of the method to the pulsars with the frequency higher than 16 Hz as shown by Dormody et al. (2011).

A model of the 8° radius circle sky patch is constructed for each of the candidates. The model includes galactic and isotropic diffuse emission components and all 3FGL sources within 8° from the position of interest. We optimize the parameters of the model with unbinned likelihood analysis by the *gtlike* tool. Normalization of the galactic and isotropic diffuse emissions and spectral parameters of the target source were considered as free parameters, while the spectral parameters of all neighboring sources were fixed at the 3FGL values. The spectral form for each source is power-law, log-parabola or power-law with exponential cutoff based on the 3FGL data. Next, using the *gtsrcprob* tool each photon is assigned a weight - probability to originate from the given pulsar candidate. For computational efficiency we keep 40000 events with the highest weights for each source. Finally, the photon arrival times are converted to barycentric frame using the *gtbary* tool.

²<http://fermi.gsfc.nasa.gov/ssc/data/access/>

3. Method

The search for pulsations is performed with the time-differencing technique first proposed by Atwood et al. (2006) and subsequently refined by Pletsch et al. (2012a). We scan over the pulsar's frequency f and spin-down rate \dot{f} using the array of barycentric photon arrival times t_a and corresponding weights w_a . First, the arrival times are corrected to compensate for frequency evolution

$$\tilde{t} = t + \frac{\gamma}{2}(t - t_0)^2, \quad (1)$$

where $\gamma = \dot{f}/f$ and $t_0 = 286416002$ (MJD 55225) is a reference epoch. The spectral density P_m is obtained with a Fourier transform of the time differences

$$P_m = \text{Re} \sum_{a,b=1} \Pi(\Delta t_{ab}/2T) w_a w_b e^{-2\pi i f_m \Delta t_{ab}}, \quad (2)$$

where $\Delta t_{ab} = t_b - t_a$, $f_m = m/T$, $T = 2^{19}$ and $\Pi(x)$ is the rectangular function which takes the value of 1 for $-0.5 < x < 0.5$ and 0 otherwise. Technically we consider only positive time differences and bin the time interval $(0, T)$ into $N = 2^{26}$ bins. Within the cycle over all event pairs one calculates the sum of product of weights $w_a w_b$ in each bin. This prepares an input for the Fast Fourier Transform performed with the open source library *fftw* (Frigo & Johnson 2005)³.

We use the same value of T as Pletsch et al. (2012a). The Nyquist frequency is $N/2T = 64$ Hz which determines a choice of N . The relatively high value of the Nyquist frequency is required to minimize the artificial binning noise keeping in mind that some pulsars may be found at the second harmonic of the frequency. We scan over the parameter γ from 0 to -1.6×10^{-11} with a step equal to -1×10^{-15} . The range corresponds to the pulsar characteristic age greater than 1 kyr. The step is selected taking into account the computation time available for the project. The value used introduces moderate loss of power for pulsations with frequencies higher than 10 Hz, see Eq. 3 of Ziegler et al. (2008).

The values of f and \dot{f} corresponding to the highest P_m are used as a starting point for the final

coherent scan. The latter is performed with maximization of the weighed H -test statistic (Jager et al. 1989) defined as follows:

$$H = \max_{1 \leq L \leq 20} \left[\sum_{l=1}^L |\alpha_l|^2 - 4(L-1) \right], \quad (3)$$

where α_l is a Fourier amplitude of the l -th harmonic

$$\alpha_l = \frac{1}{\chi} \sum_a w_a \exp^{-2\pi i l f \tilde{t}_a},$$

$$\chi^2 = \frac{1}{2} \sum_a w_a^2.$$

The maximization is performed by a scan over f and γ with the steps of 5×10^{-9} Hz and $2.5 \times 10^{-18} \text{ s}^{-1}$. The steps are chosen to ensure the coherence over the whole observation time interval. We take into account that a combination of the pulsar's frequency and an inverse Fermi orbital period T_{LAT} may be found at the semi-coherent stage. Therefore, the H -test is repeated three times starting from f , $f+1/T_{LAT}$ and $f-1/T_{LAT}$.

In this work an extensive scanning is performed and therefore a theoretical distribution of H -test statistic for the null hypothesis of non-pulsating object may not be used directly. We estimate the H distribution using the results of the scan for the 1720 3FGL objects identified as blazars, see Fig. 1. We extrapolate the tail of the distribution with the exponential function and require that the probability to have a single false candidate in the whole scan is less than 5%. Thus we arrive to the threshold value $H_{th} = 98$. Unlike the rest of the work here we used identification information to select blazars from all the sources. We note that this does not affect detection uniformity since the same H_{th} is then used for all sources. Moreover, the procedure stays conservative in case of pulsar contamination in the blazars sample. In this case the H_{th} would be overestimated and the probability of the false candidate appearance even less than required.

4. Results

There are 40 pulsars found in a blind search, see Table 1 for the complete catalog. All the

³<http://www.fftw.org>

TABLE 1
A CATALOG OF GAMMA-RAY PULSARS FOUND IN A BLIND SEARCH.

no	3FGL name	H - test	f , Hz	\dot{f} , -10^{-13} Hz s $^{-1}$	age, kyr	Pulsar name	l , deg	b , deg	$G, 10^{-11}$ erg cm $^{-2}$ s $^{-1}$	Type	Ref.
1	J0007.0+7302*	658	3.16574810	36.1543	14	PSR J0007+7303	119.66	10.46	42.6	Q	1
2	J0357.9+3206	485	2.25189503	0.6439	554	PSR J0357+3205	162.76	-15.99	6.6	Q	1
3	J0534.5+2201*	1750	29.72739783	3698.8692	1.3	Crab pulsar	184.55	-5.78	147.2	L	2
4	J0633.7+0632	866	3.36250736 \dagger	8.9973	59	PSR J0633+0632	205.10	-0.93	12.4	Q	1
5	J0633.9+1746	11253	4.21755990 \dagger	1.9518	342	Geminga pulsar	195.13	4.27	415.3	Q	3,4
6	J0659.5+1414	199	2.59796057	3.7094	111	Monogem pulsar	201.08	8.22	2.8	L	5
7	J0734.7-1558*	189	6.44573114	5.1970	197	PSR J0734-1559	232.05	2.01	4.2	Q	6
8	J0835.3-4510*	1353	11.18978060	156.0544	11	Vela pulsar	263.55	-2.79	893.0	L	7
9	J1028.4-5819	699	10.94042199 \dagger	19.2705	90	PSR J1028-5819	285.07	-0.50	25.1	L	8
10	J1044.5-5737	252	7.19264583	28.2328	40	PSR J1044-5737	286.57	1.15	13.6	Q	9
11	J1048.2-5832	147	8.08368205 \dagger	62.7274	20	PSR J1048-5832	287.43	0.58	20.1	L	10
12	J1057.9-5227	7561	5.07321957	1.5029	535	PSR J1057-5226	285.99	6.64	29.0	L	10
13	J1413.4-6205	371	9.11230510	22.9610	63	PSR J1413-6205	312.37	-0.73	19.8	Q	9
14	J1418.6-6058*	111	9.04346192 \dagger	138.3125	10	PSR J1418-6058	313.32	0.13	31.0	Q	1
15	J1429.8-5910*	101	8.63231846 \dagger	22.7099	60	PSR J1429-5911	315.26	1.32	8.8	Q	9
16	J1459.4-6053	313	9.69450009	23.7476	65	PSR J1459-6053	317.88	-1.80	11.0	Q	1
17	J1509.4-5850*	562	11.24546441	11.5913	154	PSR J1509-5850	319.98	-0.62	10.3	L	11
18	J1620.8-4928*	211	5.81616340	3.5480	260	PSR J1620-4927	333.90	0.39	18.0	Q	12
19	J1709.7-4429	3543	9.75607885	88.5318	17	PSR J1709-4429	343.10	-2.69	131.5	L	13
20	J1732.5-3130	1247	5.08792277	7.2603	111	PSR J1732-3131	356.31	1.02	14.9	Q	1
21	J1741.9-2054	5503	2.41720733	0.9926	386	PSR J1741-2054	6.41	4.90	11.8	L	1
22	J1809.8-2332	2790	6.81248050	15.9679	68	PSR J1809-2332	7.39	-2.00	44.8	Q	1
23	J1826.1-1256*	411	9.07223648 \dagger	100.0361	14	PSR J1826-1256	18.56	-0.38	41.5	Q	1
24	J1836.2+5925	756	5.77154961 \dagger	0.5005	1828	PSR J1836+5925	88.88	25.00	59.8	Q	1
25	J1846.3+0919	282	4.43357094	1.9521	360	PSR J1846+0919	40.69	5.35	2.5	Q	9
26	J1907.9+0602	210	9.37783521	76.9151	19	PSR J1907+0602	40.19	-0.90	31.9	L	1,14
27	J1952.9+3253*	122	25.29478173 \dagger	37.4774	107	PSR J1952+3252	68.78	2.83	15.1	L	15
28	J1954.2+2836*	127	10.78634243 \dagger	24.6212	69	PSR J1954+2836	65.24	0.38	10.8	Q	9
29	J1957.7+5034	349	2.66804343	0.5043	839	PSR J1957+5033	84.60	11.01	3.2	Q	9
30	J1958.6+2845	452	3.44356138	25.1308	22	PSR J1958+2846	65.88	-0.35	9.9	Q	1
31	J2021.1+3651	562	9.63902020 \dagger	89.0385	17	PSR J2021+3651	75.23	0.11	50.4	L	16
32	J2021.5+4026*	122	3.76904980 \dagger	8.1591	73	PSR J2021+4026	78.23	2.08	88.3	Q	1
33	J2028.3+3332	323	5.65907212	1.5557	576	PSR J2028+3332	73.37	-3.00	6.4	Q	12
34	J2030.0+3642	192	4.99678975	1.6231	488	PSR J2030+3641	76.13	-1.43	4.6	L	17
35	J2030.8+4416*	160	4.40392491 \dagger	1.2603	554	PSR J2030+4415	82.35	2.89	5.2	Q	12
36	J2032.2+4126	106	6.98089488 \dagger	9.9452	111	PSR J2032+4127	80.22	1.02	16.0	L	1
37	J2055.8+2539	807	3.12928985	0.4016	1236	PSR J2055+2539	70.69	-12.53	5.5	Q	9
38	J2140.0+4715*	121	3.53545109	0.2225	2520	PSR J2139+4716	92.64	-4.04	2.3	Q	12
39	J2229.0+6114*	152	19.36285105	294.8890	10	PSR J2229+6114	106.65	2.95	23.5	L	18
40	J2238.4+5903	152	6.14486843 \dagger	36.5838	27	PSR J2238+5903	106.55	0.48	5.9	Q	1

NOTE.—Frequency f and spin-down rate \dot{f} of gamma pulsations correspond to the epoch MJD 55225. Characteristic age is estimated as $-f/2\dot{f}$. The last six columns contain the object information from the literature: pulsar name, J2000 Galactic coordinates, Fermi LAT energy flux for $E > 100$ MeV (Acero et al. 2015), type (Q - radio-quiet, L - radio-loud) and a reference to the first identification of gamma pulsations. * new pulsars with respect to the catalog of the previous work (Rubtsov & Sokolova 2015). \dagger pulsars detected at the second harmonic of the frequency.

References. — (1) Abdo et al. (2009a); (2) Kniffen et al. (1974); (3) Halpern & Holt (1992); (4) Bertsch et al. (1992); (5) Ma et al. (1993); (6) Saz Parkinson (2010); (7) Thompson et al. (1975); (8) Abdo et al. (2009b); (9) Saz Parkinson et al. (2010); (10) Thompson (2008); (11) Weltevrede et al. (2010); (12) Pletsch et al. (2012a); (13) Thompson et al. (1996); (14) Abdo et al. (2010); (15) Ramanamurthy et al. (1995); (16) Halpern et al. (2008); (17) Camilo (2012); (18) Halpern et al. (2001).

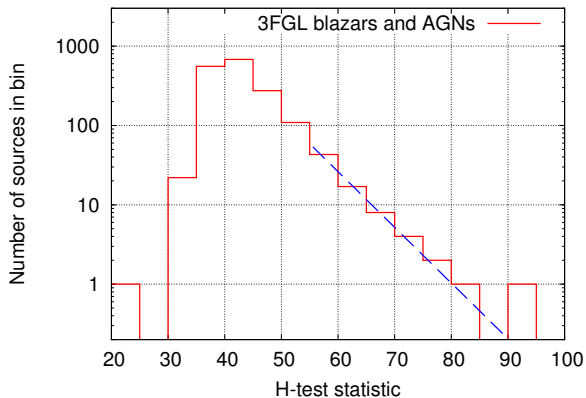


Fig. 1.— The distribution of H -test statistic for 3FGL indentified blazars

sources found in this *Paper* were known previously as gamma-ray pulsars. These include 25 radio-quiet and 15 radio-loud pulsars. There are 15 pulsars detected at the second harmonic of their frequency – these are marked with a dagger in Table 1. We note that all 25 pulsars from our previous blind search (Rubtsov & Sokolova 2015) are also found here. The blind search requires the threshold value of H_{th} to be relatively high in order to exclude possible false detections. Meanwhile, 11 known gamma-ray pulsars, namely PSR J0205+6449, PSR J0248+6021, PSR J1124-5916, PSR J1135-6055, PSR J1422-6138, PSR J1746-3239, PSR J1803-2149, PSR J1813-1246, PSR J1833-1034, PSR J1838-0537 and PSR J1932+1916, are detected with the H -test statistic between 52.5 and 98. While the correct frequency is found for these pulsars the identification is unfeasible without prior knowledge and therefore they are not included in the catalog.

We compare the distributions of the observed parameters for the radio-loud and radio-quiet pulsars with the Kolmogorov-Smirnov (KS) and Anderson-Darling (AD) tests using R (R Core Team 2013) and $kSamples$ package (Scholz & Zhu 2016). We summarize the results in Table 2 and Figures 2-7. The tests were performed. There are no statistically significant differences in characteristic age, \dot{P} , spin-down luminosity, gamma-ray luminosity and Galactic coordinates. The rotation period histograms are marginally different with pre-trial AD-probability of 4×10^{-3} . The post-trial significance is only 5% taking into ac-

count that 6 independent tests are performed with 2 different statistical methods (AD and KS).

Based on the general agreement of the observed parameters of radio-loud and radio-quiet pulsars, one may assume that the chance probability of the particular pulsar to enter the blind search catalog does not depend on its radio emission properties. Therefore the fraction of the radio-quiet pulsars in the whole population of the gamma-ray pulsars may be estimated with the corresponding fraction in the catalog:

$$\epsilon_{RQ} = \frac{N_{RQ}}{N_{RQ} + N_{RL}} = 0.63 \pm 0.08 \text{ (68\% CL)}, \quad (4)$$

where N_{RQ} and N_{RL} are numbers of radio-loud and radio-quiet non-recycled pulsars correspondingly. The result is in a good agreement with our previous work (Rubtsov & Sokolova 2015).

Given that Fermi-LAT has observed 61 radio-loud pulsars and considering ϵ_{RQ} in its general sense, we predict that there are about 104 radio-quiet pulsars within the Fermi-LAT sources for which the pulsations are detectable if the precise position and ephemerides are hypothetically known. Therefore, within these sources there are more than 50 radio-quiet pulsars with still undiscovered pulsed emission. These pulsars may be tracked when more gamma-ray data are available or with the future breakthroughs in blind search techniques.

Finally, let us compare our results with the published predictions of the emission models. The radio-quiet and radio-loud pulsar distribution with age are statistically compatible, counter to the prediction of the PC models that the radio-quiet fraction depends on age. More specifically, the $\epsilon_{RQ}^{PC} \leq 0.53$ estimated for PC models and even smaller value at ages higher than 100 kyr (Gonthier et al. 2002) are in tension with our results. On the other hand, the $\epsilon_{RQ}^{OM} = 0.65$ estimated in the OM models (Perera et al. 2013) is in perfect agreement with Eq. 4. While the catalog covers nearly half of the known radio-quiet pulsars, there is no indication of the evolution of the radio-beam solid angle proposed in Ravi et al. (2010).

Acknowledgments

We are indebted to A.G. Panin for numerous inspiring discussions. We thank V.S. Beskin,

TABLE 2
RADIO-QUIET AND RADIO-LOUD PULSAR POPULATION COMPARISON

Parameter	KS probability	AD probability
P ($1/f$)	0.8%	0.4%
\dot{P}	52%	57%
Age ($-f/2\dot{f}$)	21%	13%
Luminosity ($\sim f\dot{f}$)	3%	2%
Gamma energy flux	12%	13%
l	99%	99%
b	99%	96%

NOTE.—The KS-test and AD-test probabilities for comparison of radio-quiet and radio-loud pulsar distributions over period, its time derivative, age, spin-down luminosity, energy flux above 100 MeV and Galactic coordinates.

M.S. Pshirkov and S.V. Troitsky for useful comments and suggestions. We are obliged to the anonymous referee of The Astrophysical Journal Letters for suggesting more efficient analysis technique as a comment to our previous paper and to the anonymous referee of The Astrophysical Journal work for suggesting many improvements. The work is supported by the Russian Science Foundation grant 14-12-01340. The analysis is based on data and software provided by the Fermi Science Support Center (FSSC). We used SIMBAD astronomical database, operated at CDS, Strasbourg, France. The numerical part of the work is performed at the cluster of the Theoretical Division of INR RAS.

REFERENCES

- Atwood, W. B., Ziegler, M., Johnson, R.P., & Baughman, B.M., 2006, ApJ, 652, L49.
- Abdo, A. A., et al., 2009, Science, 325, 840.
- Abdo, A. A., et al., [Fermi-LAT Collaboration], 2009, ApJ, 695, L72.
- Abdo, A. A., Ackermann, M., Ajello, M., et al. 2010, ApJ, 711, 64.
- Acero, F., et al., [Fermi-LAT Collaboration], 2015, ApJ Suppl., 218, 23.

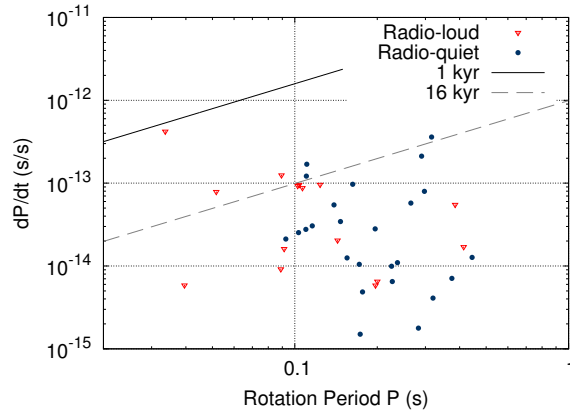


Fig. 2.— $P - \dot{P}$ plot for 40 pulsars found with a blind search in the present *Paper*. $P = \frac{1}{f}$ is a rotation period. The lines show maximum characteristics ages for present and previous blind searches.

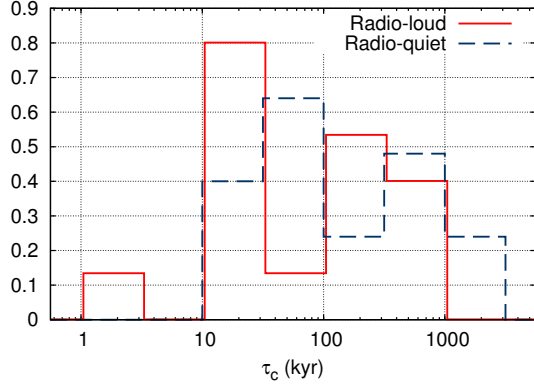


Fig. 3.— Distributions of characteristic age $\tau_c = -\frac{\dot{f}}{2f}$ for radio-loud and radio-quiet pulsars. The two distributions are compatible with KS probability 21%.

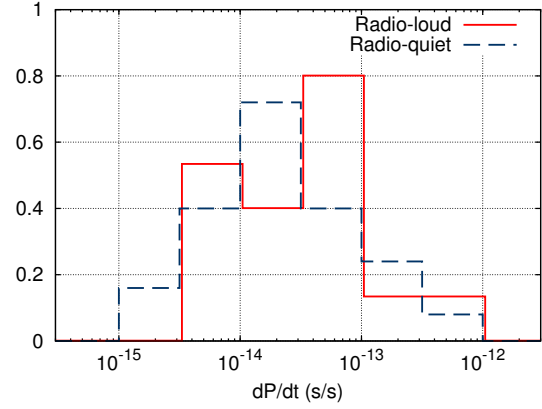


Fig. 5.— Distributions of \dot{P} for radio-loud and radio-quiet pulsars. The two distributions are compatible with KS probability 52%.

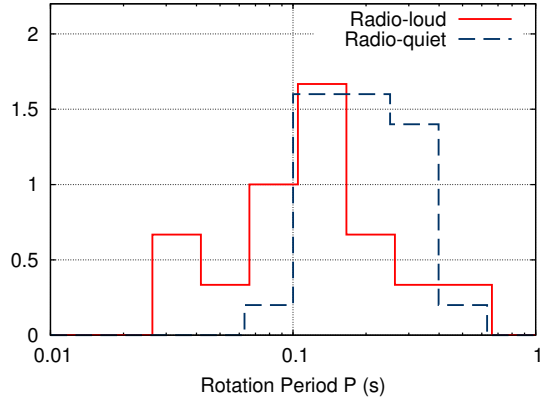


Fig. 4.— Distributions of the rotation period P for radio-loud and radio-quiet pulsars. The two distributions are compatible with KS probability 0.8%.

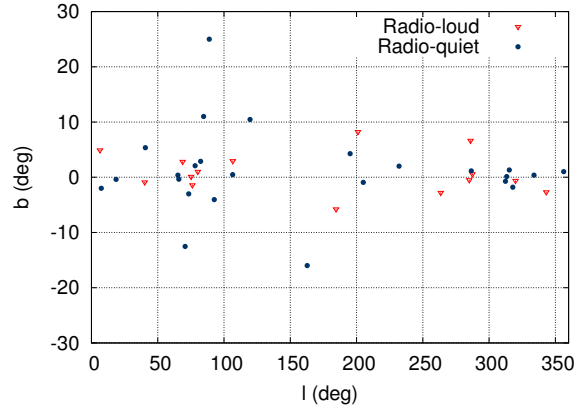


Fig. 6.— Galactic coordinates of radio-loud and radio-quiet gamma-ray pulsars

- Atwood, W. B., et al., [LAT Collaboration], 2009, *ApJ*, 697, 1071.
- Bertsch, D. L., et al., 1992, *Nature*, 357, 306-307.
- Camilo, F., 2012, *ApJ*, 746, 39.
- Caraveo, P. A., 2014, *Annual Review of Astronomy and Astrophysics*, 52.
- Cheng, K. S., Ho, C., & Ruderman, M. A., 1986, *ApJ*, 300, 500.
- Clark, C. J., et al., 2015, *ApJ*, 809, L2.
- Frigo, M., & Johnson, S. G., 2005, *Proceedings of the IEEE*, 93 (2), 216.
- Gonthier, P. L., Ouellette, M.S., Berrier, J., O'Brien, S., & Harding, A. K., 2002, *ApJ*, 565, 482.
- Ziegler, M., Baughman, B. M., Johnson, R. P., & Atwood, W. B. 2008, *ApJ*, 680, 620-626.
- Grenier, I. A., & Harding, A.K., 2015, *Comptes Rendus Physique* 16, 641.
- Halpern, J. P., & Holt, S.S., 1992, *Nature*, 357, 222-224.
- Halpern, J. P., Camilo, F., Gotthelf, E. V., Helfand, D. J., Kramer, M., Lyne A. G., Leighly, K. M., & Eracleous, M., 2001, *ApJ*, 552, L125-L128
- Halpern, J. P., et al., 2008, *ApJ*, 688, L33.
- Jager, de O. C., Raubenheimer, B. C., & Swanepoel, J.W.H., 1989, *A&A*, 221, 180.
- Kniffen, D. A., Hartman, R. C., Thompson, D. J., Bignami, G. F., Fichtel, C. E., Tumer, T., gelman, H., 1974, *Nature*, 251, 397-399.
- Ma, Y., Lu, T., Yu, K. N., Young, C. M., 1993, *Astrophysics and Space Science*, 201, 113.
- Marelli, M., Mignani, R. P., De Luca, A., Saz Parkinson, P. M., Salvetti, D., Den Hartog, P. R., & Wolff, M. T., 2015, *ApJ*, 802, 78.
- Perera, B. B. P., McLaughlin, M. A., Cordes, J. M., Kerr, M., Burnett, T. H., & Harding, A.K., 2013, *ApJ*, 776, 61.
- Pletsch, H. J., et al., 2012, *ApJ*, 744, 105.
- Pletsch, H. J., et al., 2012, *ApJ*, 755, 2012, L20.
- Ramanamurthy, P.V., et al., 1995, *ApJ*, 447, L109.
- Ravi, V., Manchester, R. N., & Hobbs, G., 2010, *ApJ*, 716, L85-L89.
- Rubtsov, G. I., & Sokolova, E.V., 2015, *JETP Lett*, 100, 689.
- Saz Parkinson, P. M., 2010, *AIP Conference Proceedings of Pulsar Conference 2010 "Radio Pulsars: a key to unlock the secrets of the Universe"*, Sardinia.
- Saz Parkinson, P. M., et al., 2010, *ApJ*, 725, 571-584.
- Sturmer, S. J., & Dermer, C.D., 1996, *A&AS*, 120, 99.
- Sturrock, P. A., 1971, "A Model of pulsars," *ApJ*, 164, 529.
- Thompson, D. J., et al., 1975, *ApJ*, 200, L79.
- Thompson, D. J., et al., 1996, *ApJ*, 465, 385.
- Thompson, D. J., 2008, *Rep. Prog. Phys.*, 71, 116901.
- Watters, K. P., & Romani, R. W., 2011, *ApJ*, 727, 123.
- Weltevrede, P., et al., [Fermi-LAT Collaboration], 2010, *ApJ*, 708, 1426.
- Dormody, M., Johnson, R. P., Atwood, W. B., et al. 2011, *ApJ*, 742, 126.
- R Core Team 2013, *R: A language and environment for statistical computing*. R Foundation for Statistical Computing, Vienna, Austria.
- Scholz, F., & Zhu, A. 2016, *kSamples: K-Sample Rank Tests and their Combinations*. R package version 1.2-4.

This 2-column preprint was prepared with the AAS L^AT_EX macros v5.2.

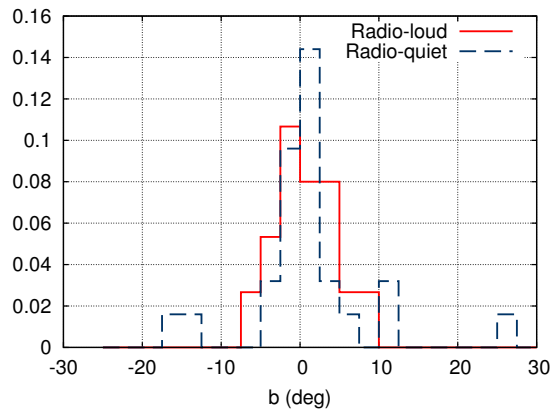


Fig. 7.— Distributions of Galactic latitude b for radio-loud and radio-quiet pulsars. The two distributions are compatible with KS probability 99%